Intelligent Vehicles Symposium 2006, June 13-15, 2006, Tokyo, Japan

Camera Calibration Method for Far Range Stereovision Sensors Used in Vehicles

Tiberiu Marita, Florin Oniga, Sergiu Nedevschi

Computer Science Department
Technical University of Cluj-Napoca
Cluj-Napoca, 400020, ROMANIA

Thorsten Graf, Rolf Schmidt

Electronic Research
Volkswagen AG
Wolfsburg, 38436, GERMANY

Abstract

This paper presents a camera calibration method for far-range stereo-vision used for driving environment perception on highways. For a high accuracy stereovision system the most critical camera parameters are the relative extrinsic parameters which are describing the geometry of the stereo-rig. Experiments proved that even a few seconds drift of the relative camera angles can lead to disastrous consequences in the whole stereo-vision process: incorrect epipolar lines and consequently lack of reconstructed 3D points. Therefore we propose an off-line method able to give a very accurate estimation of these parameters and on-line methods for monitoring their stability in time taking into account the real-world automotive conditions, which can introduce drifts to the initial parameters due vibrations, temperature variations etc.

1 Introduction

Optical sensors, such as visible-light cameras, are usually referred to as passive sensors because they acquire data in a non-intrusive way. They are low cost sensors but do not perform direct measurements as the active ones. The measurement is done indirectly from the 2D image and this process could be time consuming and its accuracy dependents on the vision sensor setup. However, the use of a high resolution, high accuracy stereovision algorithm provides accurate results in 3D estimation while delivering a larger amount of data, thus making some obstacle detection tasks as grouping and tracking easier, and allowing a subsequent classification of the obstacles. Moreover, the lane detection is a key problem in any driving assistance system, and one of the privileges of computer vision. The measuring capabilities of vision sensors with monocular cameras are reduced because are relying on some prior knowledge of the scene as flat road assumption or constant pitch angle, which cannot be met in real scenarios. With stereo-vision systems the full 3D reconstruction of the scene is possible, but a high accuracy of the camera parameters is required.

The calibration of a stereovision system deals with the estimation of the following parameters:

- *Internal parameters of the stereo-rig*: intrinsic parameters (focal length and the principal point position) and relative position and orientation of the two cameras (relative extrinsic parameters).
- *Absolute extrinsic parameters of the stereo-rig*: position and orientation of the stereo-rig (usually the left camera coordinate system) relative to a world coordinate system in which the measurements are reported.

The quality of the internal parameters is influencing the accuracy of the essential and fundamental matrix and consequently the positions of the epipolar lines [1] which are essential in the stereo correlation process. Their wrong estimation can lead to lack of correlated points or false correlations with disastrous consequences for the whole stereo reconstruction process. The quality of the absolute extrinsic parameters is linked to the position of the reconstructed 3D points in the world coordinate system.

Regarding the intrinsic parameters calibration there are many general purpose methods found in the literature [2]-[5]. Most of them are estimating the parameters by minimizing the projection error of a set of control points from a calibration object/pattern with known structure against their detected 2D

image positions. Multiple views of the calibration object are taken and the accuracy of the results usually increases with the total number of control points. A special note must be mentioned for the Bouguet method implemented in the Caltech Camera Calibration Toolbox [5], which was intensively tested and used in our experiments for the estimation of the intrinsic parameters.

Regarding the extrinsic parameters estimation, the principle is the same: minimizing the projection error of some 3D control points with known positions in the world coordinate system (measurement coordinate system). General purpose methods [5], [6] are using the same calibration object as for the intrinsic parameters estimation. These approaches can be satisfactory for monocular or near range indoor applications, but are completely unsuited for far range stereo-vision (because in the estimation process the error was minimized for a small calibration object and for near distances). Therefore, using a calibration scene with sizes comparable with the working range of the stereo reconstruction application has been proved a reliable solution. Such methods [8], [9] are using as control points, painted markers on a flat surface of a few meters or tens of meters in length.

In this paper we present a method for estimating the extrinsic camera parameters suited for far range and high accuracy stereo-vision. As control points, 'X'-shaped targets are placed vertically in a flat calibration scene, up to 40 m in depth. The 3D coordinates of the targets' are measured in the world coordinate system. Each camera is calibrated individually (so the method can be applied also for mono systems). The 2D image projections of the targets' central points are detected automatically and the projection error of their 3D coordinates are minimized against the position and orientation of the camera in the world coordinate system using the Gauss-Newton method. The obtained results proved to be very accurate regarding both the absolute extrinsic parameters of each camera individually and especially for the relative extrinsic parameters, allowing a very accurate stereo reconstruction procedure. Furthermore, two original methods for on-line self checking of the stereo system geometry are proposed. These methods are allowing monitoring the stability of the internal parameters in time taking into account the real-world automotive conditions, which can introduce drifts to the initial parameters due vibrations or temperature variations.

2 Camera Model

The intrinsic parameters of each camera are the *principal point*'s position (x_c, y_c) [pixels], the *focal length* of the camera f [pixels] and the first two radial (*k1, k2*) and tangential (*p1, p2*) distortion coefficients [4], [5]. The intrinsic parameters are assumed to be correctly computed, using the algorithm presented in [5].

The stereovision sensor consists in two cameras mounted on a rigid frame (stereo-rig). The position and orientation of the cameras' are completely determined by the absolute extrinsic parameters: the translation vectors $\mathbf{T}_L$ and $\mathbf{T}_R$ (1), and the rotation matrices $\mathbf{R}_L$ and $\mathbf{R}_R$ (2) relative to the world coordinate system which coincides with the ego-car coordinate system. The car/world coordinate system has its origin on the ground in the front of the car, and its Z axis points in our direction of travel (fig. 1). The relative extrinsic parameters can be computed from the absolute ones (3).

$$\mathbf{T} = [X_{cw}, Y_{cw}, Z_{cw}]^{\mathrm{T}} \tag{1}$$

$$\mathbf{R} = \begin{vmatrix} r_{11} & r_{12} & r_{13} \\ r_{21} & r_{22} & r_{23} \\ r_{31} & r_{32} & r_{33} \end{vmatrix} \tag{2}$$

$$\begin{cases} \mathbf{T}_{rel} = \mathbf{R}_L^T \cdot (\mathbf{T}_R - \mathbf{T}_L) \\ \mathbf{R}_{rel} = \mathbf{R}_L^T \cdot \mathbf{R}_R \end{cases} \tag{3}$$

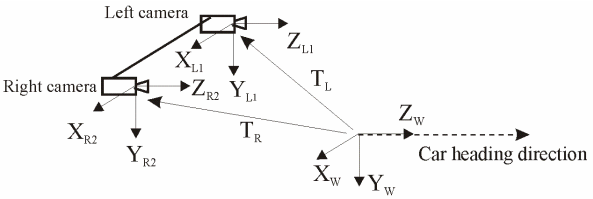

Fig. 1. The cameras' and the car coordinate systems.

3 Extrinsic Parameters Calibration

3.1 The calibration scenario

A calibration scenario on a flat surface of 30–40 m depth and 5–10 m width was chosen (fig.4). As control points a set of 'X'-shaped targets were placed vertically in a calibration scene,

There are some aspects influencing the quality of the obtained extrinsic parameters which were taken into account when setting up this calibration scenario:
- the 3D control points should be uniformly spread over the calibration field;
- their 3D coordinates should be measured as accurate as possible;
- the projection of the control points onto the image plane should be easily detected with sub-pixel accuracy.

The 'X'-shape of the targets was chosen due to some major advantages in the automated detection process:
- it has a low rate of false targets detections because most of the structures in our 3D scenarios are '+'-shaped structures (due to predominance of horizontal and vertical features) while the 'X'-shape is based on oblique features;
- the center of the target can be easily computed;
- the centers of the vertical 'X'-shaped targets are more easier to detect than lines or other markers painted on the road [8[, [9], which are poorly visible at long distances due to perspective projection effects, especially when the cameras are mounted at low pitch angles as in vehicles.

3.2 Correction of the lens distortion effects

First, a correction algorithm is applied to remove the lens distortion effects encoded in the four distortion coefficients using the distortion model of the cameras [3], [5]. This is a compulsory step science targets which are far from the image center can suffer a distortion drift up to a few pixels, depending on the quality and geometry of the lenses. The destination un-distorted images are obtained by remapping the original images to the undistorted coordinates using bilinear interpolation. The correction of the lens distortion simplifies the projection model of the 3D points onto the image plane used in the extrinsic parameters estimation. The lens distortion correction is applied also on every processed image in the stereo-reconstruction application.

3.3 Automatic detection of the targets 2D image projections

Detection of the targets is performed in 3 stages using multiple validation constraints in order to eliminate false positives which can occur in some scenes with non-uniform background.

1. First, the grayscale image is segmented using an automated global threshold detection method [7] computed in the region of interest (the smallest rectangle delimiting the image area occupied by the 'X'-shaped targets). Then concavities of the black areas are searched (fig. 2) and groups of four concavities (left/right/upper/lower) are formed and marked based on vicinity criteria.

Fig. 2. Concavities detection: zoomed area – upper/lower/ left/right concavities; complete image – centers of detected groups of 4-concavities are marked.

2. Validation by searching oblique edge points obtained with the Roberts-cross operator in the neighborhoods of the previously found concavities. The areas occupied by oblique edge points around each concavity is marked (fig. 3) and used in the next validation stage.

Fig. 3. Validation by oblique edges.

3. A final validation step is performed by applying a classical pattern-matching method with synthetically generated 'X'-shaped patterns of different sizes in the surrounding region of the already found targets. The final results of the targets detection are shown in figure 4.

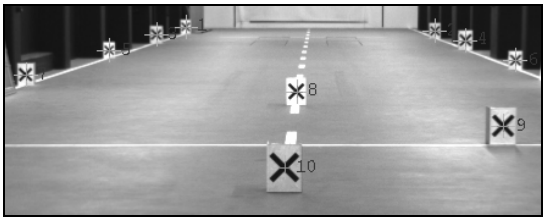

Fig. 4. Calibration scenario - the 3D control points are situated in the centers of the 'X'-shaped targets.

To detect the sub-pixel position of the targets' center, the image area bounding the current target is zoomed-in using bi-cubic interpolation (fig. 5-left). To detect the target's center position along the *X* axis, the sum of the pixel values along each column is computed (fig. 5-center). The maximum of these sums is considered (in the center of the target the number of light pixels along the row and the column is maximal). To minimize the influence of noise and image discrete nature, instead of considering exactly the position of the maximum, we take the mid point of the interval having values above 90% from the maximum. The computed position is now mapped back by downscaling and translation to the original image coordinates. To detect the target's center position along the *Y* axis the procedure is similar, except that it's applied along the vertical direction (fig. 5-right).

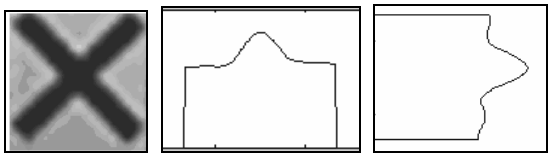

Fig. 5. Zoomed 'X-shape' image (left); The sum of intensities along the columns for each row (center); The sum of intensities along the rows for each column (right).

3.4 Estimation of the extrinsic parameters

Considering a known 3D point $P_A(X_A, Y_A, Z_A)$ and its image projection $p(x_i, y_i)$, due to perspective projection [1], the following relations are available:

$$\begin{cases} x_i - x_c = -f \dfrac{r_{11}(X_A - X_{cw}) + r_{21}(Y_A - Y_{cw}) + r_{31}(Z_A - Z_{cw})}{r_{13}(X_A - X_{cw}) + r_{23}(Y_A - Y_{cw}) + r_{33}(Z_A - Z_{cw})} \\ y_i - y_c = -f \dfrac{r_{12}(X_A - X_{cw}) + r_{22}(Y_A - Y_{cw}) + r_{32}(Z_A - Z_{cw})}{r_{13}(X_A - X_{cw}) + r_{23}(Y_A - Y_{cw}) + r_{33}(Z_A - Z_{cw})} \end{cases} \quad (4)$$

For each known 3D point there are two equations involving the 12 unknowns. The 9 unknowns representing the rotation matrix have only 3 freedom degrees (represented by the 3D angles of rotation) Thus it is necessary to add several constraints that model the dependencies between the rotation matrix coefficients. These constraints are obtained easily considering the fact that the rotation matrix is orthogonal [1], and therefore six equations can be supplementary added:

$$\begin{cases} r_{11} \cdot r_{11} + r_{12} \cdot r_{12} + r_{13} \cdot r_{13} - 1 = 0 \\ r_{21} \cdot r_{21} + r_{22} \cdot r_{22} + r_{23} \cdot r_{23} - 1 = 0 \\ r_{31} \cdot r_{31} + r_{32} \cdot r_{32} + r_{33} \cdot r_{33} - 1 = 0 \\ r_{11} \cdot r_{21} + r_{12} \cdot r_{22} + r_{13} \cdot r_{23} = 0 \\ r_{11} \cdot r_{31} + r_{12} \cdot r_{32} + r_{13} \cdot r_{33} = 0 \\ r_{21} \cdot r_{31} + r_{22} \cdot r_{32} + r_{23} \cdot r_{33} = 0 \end{cases} \quad (5)$$

By using a number $n>=3$ of 3D control points, from (4) and (5) a non-linear system of $2n+6$ equations is built (7), where the first $2n$ equations are obtained by applying (5) for each control point, and the last 6 equations are the constraints defined in (5):

$$\mathbf{F}(u) = 0 \quad (6)$$

where u is a vector of the 12 unknowns (X_{cw}, Y_{cw}, Z_{cw}, r_{ij}), for $i, j = 1,2,3$.

To solve this system, the Gauss-Newton iterative method was used. This method starts from an initial random solution (the constraint that the initial solution must be close to the real one is not required), and converges applying iteratively correction steps. As initial solution the translation vector was set to the null vector and the rotation matrix to the identity matrix. Suppose that, after a number of correction steps, the current solution is u_i and, by applying another correction step, the new

solution is $u_{i+1} = u_i + du$, than the residual du is obtained by solving the system:

$$\mathbf{J} \cdot du = \mathbf{F} \tag{7}$$

where $\mathbf{J}$ is the Jacobian matrix associated to equation system $\mathbf{F}(u) = 0$.

To solve the over-determined system (7) a least-squares method was used (8). The decision to stop the correction process after a number of iterations is taken when the norm of the residual du is smaller than a threshold.

$$du = u_{i+1} - u_i = -\left(\mathbf{J}(u_i)^T \cdot (\mathbf{J}(u_i)\right)^{-1} \cdot \mathbf{J}(u_i)^T \cdot \mathbf{F}(u_i) \tag{8}$$

4 On-line Self-Checking of the Stereo-Rig Internal Parameters

Real-world automotive conditions, can lead to drifts to the initial camera parameters due vibrations, temperature variations etc. Therefore some methods used to check the geometry of the stereo-rig during exploitation would be very useful. The checking should be applied from time to time and should not require a specific calibration scene. In the following two such methods which can be used on-line during the exploitation of the stereovision sensor are proposed.

4.1 Self-checking using infinity points

It is very likely that on highway or country roads to have a visible horizon line. Usually the mid points of the detected horizon line are at far distance (a few hundred meters) and can be considered at infinity in comparison with the depth range of the stereovision sensor (<100 m). Thus, these points can be considered in a plane situated at infinity. Let consider the disparity equation for points situated at infinity:

$$\mathbf{m}_R = \mathbf{H}_\infty \cdot \mathbf{m}_L = \mathbf{A}_R \cdot \mathbf{R}_{rel} \cdot \mathbf{A}_L^{-1} \cdot \mathbf{m}_L \tag{9}$$

The above equation says that for the left image projection ($\mathbf{m}_L$) of a point at infinity, its correspondent ($\mathbf{m}_R$) in the right view can be obtained using the homography matrix of the plane at infinity $\mathbf{H}_\infty$, which depends only on the internal parameters of the stereo rig: the intrinsic parameters of the two cameras encoded in the two intrinsic matrices $\mathbf{A}_L$ and $\mathbf{A}_R$ [3] and the relative rotation between the two cameras $\mathbf{R}_{rel}$.

By setting the homogeneous coordinates of the point $\mathbf{m}_L$ to 0 in (9) we define the *expected disparity* of infinity points as:

$$\mathbf{d}_\infty = \begin{bmatrix} d_x \\ d_y \\ 1 \end{bmatrix} = \mathbf{A}_2 \cdot \mathbf{R} \cdot \mathbf{A}_1^{-1} \cdot \begin{bmatrix} 0 \\ 0 \\ 1 \end{bmatrix} \tag{10}$$

The method computes the expected disparity for the camera parameters in use. When we want to check if the stereo-system's geometrical configuration fulfils the initial values we compute the average disparity for a set of horizon points: d_{avg} (if a valid horizon line is available):

$$\mathbf{d}_{avg} = \left\langle \left\| \begin{bmatrix} x_i^R \\ y_i^R \end{bmatrix} - \begin{bmatrix} x_i^L \\ y_i^L \end{bmatrix} \right\| \right\rangle \tag{11}$$

Then, if the difference between the computed average disparity of the horizon points and the expected disparity is below a threshold, we can say that the geometrical configuration is unchanged. If it is above the threshold then a geometrical change in the parameters of $\mathbf{A}_L$, $\mathbf{A}_R$ or $\mathbf{R}_{rel}$ has occurred (12). The proper value of the threshold value is determined experimentally.

$$\delta\mathbf{d} = \left| \mathbf{d}_{avg} - \mathbf{d}_\infty \right| = \begin{cases} < Trashold : Geometry\_OK \\ > Trashold : Geometry\_Wrong \end{cases} \tag{12}$$

The horizon points are matched between the left and right horizon line segments detected as the lower borders of the sky regions. The classical way to find the right image correspondents of left image features is the stereo-matching using epipolar geometry constraints [1]. But in our case this approach is not applicable because infinity points have "zero" disparity and we assume that the camera geometry might be changed (and therefore epipolar constraints

are not valid any more). Therefore a set of horizon points are selected from the left image and their correspondents in the right are found using the following algorithm:

1. Features selection in both left and right horizon lines segments which are local extreme points of the horizon line segments (local minima or maxima in the vertical direction).
2. For every feature from the left image a window based matching is performed on the set of right image features and the feature pair of the best match is selected.

4.2 Self-checking using epipolar line constraints

A measure of the stereo system's wrong geometry can be the average vertical drift from the true position of the computed epipolar line in the right image. Considering the theory of the fundamental matrix [1], it easy to deduce that the epipolar lines will have a vertical drift when small modifications are present in the focal lengths, the vertical coordinate of the principal points (1-2 pixels), the relative pitch angle of the two cameras (0.02-0.05 degrees), or large modifications of the other parameters.

Usually, when a drift appears, the effect on reconstruction is a decrease in the number of 3D points. Therefore the drift can be checked by setting different values of drift in between -2...+2 pixels with a step of 0.25, and testing the variation of the number of 3D points (as in fig. 6). The algorithm for computing the epipolar drift is described bellow:

1. For each drift value, the histogram of the number of the reconstructed 3D points is computed (only edge points were considered).
2. The maximum value of the histogram is determined.
3. Because it is not a strong maximum, a region is taken around the maximum for values higher then 95%.
4. The middle of the interval is considered as the correct position for the correspondent drift.

For a good calibrated system the drift should have values between -1 … +1 pixel. Outside this range the errors of the stereo correlation process are dramatically increasing. Considering the measurements' error range (witch is proportional with the matching accuracy ≈ 1/4 pixels) a maximum allowed drift range of -0.7 ... +0.7 is considered. If a small de-calibration appears, than the drift will have higher values (more than 1 pixel absolute values).

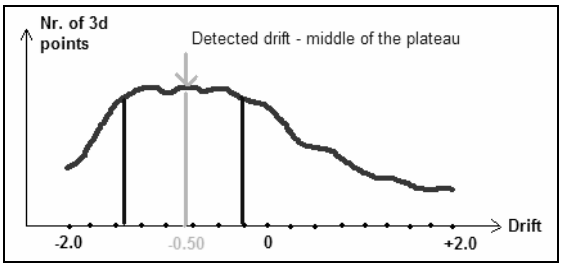

Fig. 6. Detection of the epipolar drift

5 Results

The calibration method was tested in a large number of experiments with various types of stereovision systems: from individual high quality mega-pixel CCD cameras mounted on a rigid rig to integrated stereo-heads with CMOS sensors.

The intrinsic parameters of each camera were calibrated individually. The parameters were estimated using the Bouguet's algorithm [5] by minimizing the projection errors of a set of control points placed on a coplanar calibration object viewed from different positions. Accuracy of the obtained parameters was depending on several factors: number of views, number of control points on each view, size of the calibration object, coverage of the views by the calibration object, accuracy and planarity of the calibration object etc. By using the proper calibration methodology, the obtained uncertainties of the intrinsic parameters were below one pixel. Regarding the stability of the intrinsic parameters in time the parameters remained unchanged during in-vehicle exploitation of the stereo system in a period of over 2 years.

The extrinsic parameters of each camera were calibrated using the above presented method. The accuracy of the automated targets' center detection

method was compared with the positions of hand extracted points (using a zoomed window applied on the targets). The obtained average error was bellow 0.1 pixels. The uncertainties for the extrinsic parameters roughly estimated from the residual of the Gauss-Newton minimization method were usually below 10^{-9} for the terms of **T** and 10^{-11} for the terms of **R**.

The overall accuracy of the estimated parameters was assessed offline, by measuring the reconstruction errors of 'X'-shaped targets, placed in known 3D coordinates (similar to fig. 4). The targets centers were computed with sub-pixel accuracy using the above described algorithm. In such a setup, the only errors' sources were the sub-pixel detection errors of the targets' center (about 0.1 pixels accuracy) and the targets' 3D measuring errors. The error plots of the reconstructed coordinates for one of the calibration experiments are shown in figure 7. The lateral offset errors were below 4 cm, the height errors were below 1 cm and the depth errors were below 22 cm (below 5% relative errors).

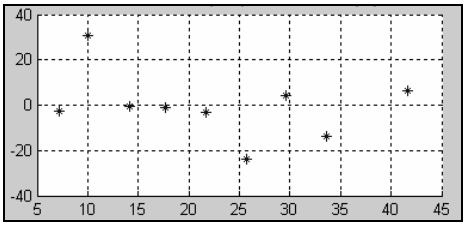

a. X errors

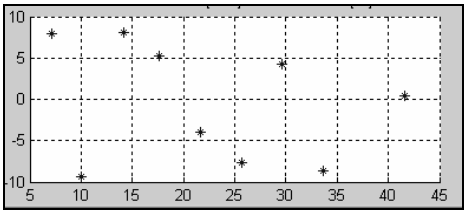

b. Y errors

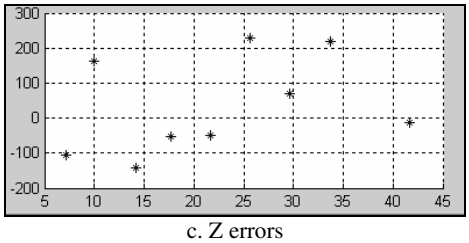

c. Z errors

Fig. 7. Absolute errors of the reconstructed control points expressed in [mm] vs. the depth of the control point [m].

The same scenario was used to validate the self-checking method based on epipolar line constraints. From the sub-pixel left-right image coordinates of the detected targets' centers an average vertical epipolar drift was computed and compared with the drift measured with the on-line method. The errors were below 0.1 … 0.2 pixels.

Regarding the self-checking method of the camera geometry by using the infinity points' constraints, for the proper estimation of the error threshold (12), the following study was made: a set of good calibration parameters was taken as reference and the expected infinity disparity $\mathbf{d}_\infty$ for the initial set of parameters computed. Then the value of each internal parameter was modified around the initial value to simulate changes in the stereo system geometry (table I).

TABLE I
SIMULATED DISPARITY ERRORS: $\delta\mathbf{d}$

Parameter	**Simulated drift**	$\delta\mathbf{d}$ [pixels]
Principal point	1 pixel	1
Focal length	10 pixels	0.2
Rotation angle	0.1 deg	2

By assuming that we have the following uncertainties in the estimation of system parameters: 1-2 pixels for principal point and focal length, 0.01 [deg] for the relative camera angles and 1 pixel in the detection of horizon points' positions, we can consider the threshold value of $\delta\mathbf{d}$ as the sum of the consequences of all these uncertainties obtaining an approximate value of $[2, 2]^T$ [pixels].

The self-checking method using infinity points' constraints was tested on different scenarios. If a proper horizon line was detected (beyond 100m, with enough local maxima) the method proved to be reliable providing for a good calibrated system an average disparity of infinity points very close to the expected one.

The calibration parameters were tested in a stereovision based lane and obstacle detection application for traffic environment perception in highway scenarios [11-13]. The system was able do

detect and track objects in a range up to 100m with a depth errors up to 5%. For comparison, the results of the extrinsic parameters calibration method from [5] were tested but the current approach has been proved far more accurate and reliable.

6 Conclusions

A dedicated calibration method for far range stereo-vision was developed. The method performs the estimation of the camera's absolute extrinsic parameters with high accuracy. Consequently, very accurate relative extrinsic parameters of the cameras' are determined, allowing a precise estimation of the epipolar lines (≈ 0 pixel drift) with benefic effects for the whole stereo reconstruction. Therefore the method is suited for the calibration of any stereo-vision system used for far range 3D reconstruction as outdoor robot vision applications or vision based driving assistance systems.

Also a set of original methods for on-line self-checking of the stereo rig internal parameters was proposed. These methods are allowing the on-line monitoring of the stability of the internal parameters during time taking into account the real-world automotive conditions, which can introduce drifts to the initial parameters.

Further work will be focused on developing an auto-calibration method of the stereo rig absolute extrinsic parameters, by knowing the internal parameters calibrated off-line and taking the advantages of available stereo reconstruction of road features in the stereo-rig coordinate system.

References

[1] E. Trucco, "Introductory techniques for 3D Computer Vision", *Prentice Hall*, 1998.

[2] Tsai, R. Y.(1987), "A versatile camera calibration technique for high-accuracy 3D machine vision metrology using off-the-shelf TV cameras and lenses". *IEEE Journal of Robotics and Automation*, RA-3(4)/1987: pp.323-344.

[3] Zhang Z (1999), "Flexible Camera Calibration By Viewing a Plane From Unknown Orientations." *International Conference on Computer Vision (ICCV'99)*, Corfu, Greece, September 1999, pp. 666-673

[4] Heikkila, J.; Silven, O. (1997), "A four-step camera calibration procedure with implicit image correction," *Proc. IEEE Computer Society Conf.*, 1997 pp.1106 –1112.

[5] J.Y. Bouguet, Camera Calibration Toolbox for Matlab, www.vision.caltech.edu/bouguetj.

[6] N. Kämpchen, , U. Franke, R. Ott, "Stereo vision based pose estimation of parking lots using 3D vehicle models", *IEEE Intelligent Vehicle Symposium*, 2002, pp. 459- 464.

[7] R.C. Gonzales, R.E. Woods, Digital Image Processing, 2-nd edition, *Prentice Hall*, 2002.

[8] S. Ernst, C. Stiller, J. Goldbeck, C. Roessig, "Camera Calibration for Lane and Obstacle detection", *IEEE Inteligent Transportation Systems*, 1999, pp. 356-361.

[9] A. Broggi, M. Bertozzi, A. Fascioli "Self-Calibration of a Stereo Vision System for Automotive Applications", *IEEE Conf. on Robotics and Automation*, Seoul, Korea, May 2001, vol.4, pp. 3698-3703.

[10] C. Zeller, O. Faugeras, Camera Self-Calibration from Video Sequences: the Kruppa Equations Revisited, *Technical Report No. 2793, INRIA*, 1996.

[11] S. Nedevschi, R. Schmidt, T. Graf, R. Danescu, D. Frentiu, T. Marita, F. Oniga, C. Pocol, "High Accuracy Stereo Vision System for Far Distance Obstacle Detection", *IEEE Intelligent Vehicles Symposium,* Parma, Italy, June 14-17, 2004, pp.161-166.

[12] S. Nedevschi, R..Schmidt, T. Graf, R. Danescu, D. Frentiu, T. Marita, F. Oniga, C. Pocol, "3D Lane Detection System Based on Stereovision", *IEEE Intelligent Transportation Systems Conference,* Washington, USA, October 4-6, 2004*,* pp. 292-297.

[13] S. Nedevschi, R. Danescu, T. Marita, F. Oniga, C. Pocol, S. Sobol, T. Graf, R. Schmidt, "Driving Environment Perception Using Stereovision", *IEEE Intelligent Vehicles Symposium,* June 2005, Las Vegas, USA, pp.331-336.